Available online at www.sciencedirect.com
ScienceDirect
Polymer 49 (2008) 809–815
polymer
www.elsevier.com/locate/polymer

# Numerical study on electrophoretical stretching dynamics of DNA in microcontraction

Zuo Chun-Cheng[1], Ji Feng*, Cao Qian-Qian[2], Yang Jing-Song[3]

*College of Mechanical Science and Engineering, Jilin University, Changchun 130025, China*

Received 7 June 2007; received in revised form 10 December 2007; accepted 10 December 2007
Available online 23 December 2007

**Abstract**

Brownian dynamics simulations are used to characterize the electrophoretical stretching process of long T4 DNA in microchannels. When DNA is forced to move through the microchannels, the pure elongational flow generated by electric field gradients in hyperbolic contraction will unravel the molecules of DNA. The effects of hydrodynamic interactions, the strain rate, the Brownian fluctuation, and the initial states of molecules on the stretching dynamics are analyzed in this paper. The computational results show us the weak dependence of polymer dynamics on hydrodynamic interactions in microcontractions. In the case of low Deborah number, the stretching process of a molecule depends on the Brownian fluctuation. However, in the case of high Deborah number, the individualistic stretching behavior can be traced to variations in the starting conformation.


*Keywords:* DNA; Brownian dynamics simulations; Stretching dynamics

## 1. Introduction

The study of stretching large DNA is of significant interest to researchers and scientists in the fields of gene mapping. It is known that the large DNA appears to be of random coiled conformation in a solution. The coiled polymer must be unwound and stretched so that the direct linear analysis can be performed. Compared with traditional approaches, the linear measurement technology promises the high-throughput genome characterization and preserves haplotype information.

Many experimental approaches have been developed during the past decade to systematically study the stretching of DNA in many microfluidic/nanofluidic geometries. These approaches can be classified as nine types as follows: (I) operating DNA with optical tweezers [1,2], magnetic tweezers [3] and optical fiber [4]; (II) extending DNA attached to a surface and digested with a restriction enzyme [5–9]; (III) confinement elongation of DNA in nanofluidic devices [10–12]; (IV) stretching of a single polymer in a uniform flow [13]; (V) unwinding of DNA in velocity gradients induced by channel contraction or expansion in a hydrodynamic flow [14–16]; (VI) the dynamics of isolated DNA molecules under hydrodynamic focusing of multiple streams [17]; (VII) electrophoretic stretching of DNA in uniform electric fields [18]; (VIII) single polymer deformation in electric field gradients created by obstacles [19,20] or microcontractions [21]; (IX) stretching of DNA under alternating current field [22–25].

To complement experimental researches, analytical studies [26–28] as well as numerical techniques such as Brownian dynamics [29–40] and Monte Carlo simulations [41] have been developed to gain deep insight into the microscopic dynamics of semiflexible polymers. These theoretical, experimental and numerical investigations extended our understanding of stretching dynamics of DNA in microchannels or nanochannels. However, to what extent hydrodynamic interactions, the Brownian fluctuation, the initial conformation, and the strain rate have

* Corresponding author. Tel.: +8613019229680; fax: +8643185095288.
*E-mail addresses:* zuocc@jlu.edu.cn (Z. Chun-Cheng), jifeng0203@hotmail.com (J. Feng), caoqianqian@email.jlu.edu.cn (C. Qian-Qian), yjs@cust.edu.cn (Y. Jing-Song).
[1] Tel.: +8613159645056; fax: +8643185095288.
[2] Tel.: +8613654373554; fax: +8643185095288.
[3] Tel.: +8613654373554; fax: +8643185095288.

0032-3861/$ - see front matter © 2007 Elsevier Ltd. All rights reserved.
doi:10.1016/j.polymer.2007.12.013

effect on electric field gradient needs to explore further, although some experimental results have been presented [21].

In this paper, we have attempted to critically examine the electrophoretic stretching of DNA in hyperbolic microchannels, stressing on the influences of hydrodynamic interactions, the Brownian fluctuation, the initial conformation, and the strain rate on the degree of DNA stretching. Relevant theoretical background is presented in Section 2, followed in Section 3 by a description of our numerical model. Results and discussions are presented in Section 4, with conclusions given in Section 5.

## 2. Theoretical background

Long polymers such as T4 DNA, with counter length $L$ much larger than the persistence length $l^p$, tend to be in coiled state in a solution. When an electric field is applied on the both ends of a microchannel, DNA molecules can be driven electrophoretically through the hyperbolic structure shown in Fig. 1. Similar to the hydrodynamic force field gradients, the electric field gradients created by hyperbolic contraction also can stretch DNA.

Without the local rotation, the electrophoretic deformation is always pure elongation [20]. It is known that, in pure hydrodynamically elongational flow, the competition between hydrodynamic friction across the polymer, which inclines to unwind the polymer, and the entropic elasticity, which tends to coil the polymer, determines the stretching rate. The Deborah number (De), $\mathrm{De} = \dot{\varepsilon}\tau$, can be used to scale the relation between the longest relaxation time $\tau$ and the inverse of strain rate $1/\dot{\varepsilon}$. The threshold value of De is 0.4 [42, 43] and the theoretical prediction may be 0.5 [44]. As De is lower than the threshold value, the polymers are in coiled states due to the dominant elasticity. When De increases to the threshold value, the conformation can transit from the coiled state to the stretched state with the competing effects counteracted each other. As De is higher than the threshold value, the preeminent hydrodynamic friction force leads to the affine deformation of polymer with the fluids until the introduction of nonlinear elasticity limits and intramolecular constraints.

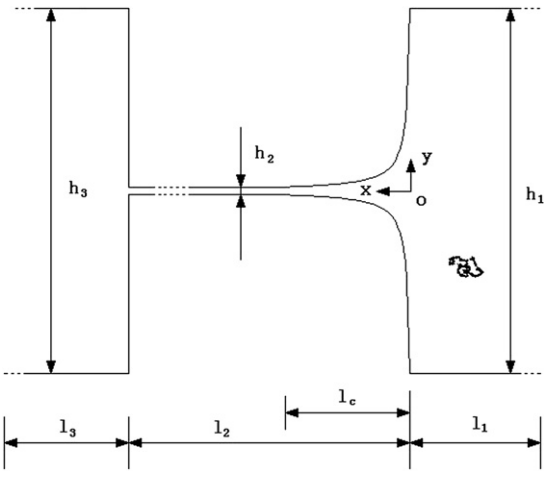


Fig. 1. A schematic diagram of the hyperbolic contraction microchannel used in the simulations. The hyperbolic equation can be expressed as: $y = c/(x + 2c/h_1)$. Here, $c = 155\ \mu\mathrm{m}^2$. DNA is driven by an electric field into the microchannel from the right side, then through the hyperbolic contraction, and out of the microchannel from the left side.

To explore the polymer deformation in electric field gradients, the effect of electric force must be concluded besides hydrodynamic friction and elasticity. Based on both the conformation-independent mobility and the local balance between electric forces and hydrodynamic forces on the polyelectrolyte, Long et al. have introduced the approximate theory of hydrodynamic equivalence [45,46]. They state that the deforming manner of DNA in an electric field $\mathbf{E}$ will be same as that in a hydrodynamic flow of velocity $\mu E$, where $\mu$ is the electrophoretic mobility. The experimental data on the steady stretching of DNA in constant electric field have also been presented by Frerree and Blanch to prove the electro-hydrodynamic equivalence [18].

With the above theoretical approximation, we seek to numerically explore the stretching process of T4 DNA in hyperbolic microchannels.

## 3. Numerical model

### 3.1. Problem setup and governing equations

A schematic diagram of the hyperbolic contraction microchannel is shown in Fig. 1. The $h_1$, $h_2$, and $h_3$ represent the widths of inlet, hyperbolic contraction and outlet, respectively. The $l_1$, $l_c$, $l_2$, and $l_3$ are used to represent the lengths of inlet, transitional region, hyperbolic contraction and outlet, respectively. An electric field is applied to drive T4 DNA into the microchannel from right side, then through the hyperbolic structure modeled by equation $y = c/(x + 2c/h_1)$, and out of the microchannel from the left side. With the Dirichlet conditions at both ends and Neumann conditions at walls specified, we use finite element method to numerically solve the Laplace equation for electric potential. Compared with the general triangle meshes in the inlet and outlet regions, the meshes on the hyperbolic contraction must be refined due to sharper gradient of electric potential. Incomplete LU preconditioner and general DMRES linear system solver are used as solution schemes. Actually, the electric field at each bead's positon used in our Brownian dynamics scheme can be calculated by interpolation among the values of surrounding elements.

T4 DNA is modeled as $N$ beads connected by $N_s = N - 1$ entropic springs. Brownian dynamics simulation with hydrodynamic interactions is first introduced by Ermak and McCammon [47]. The velocity for bead $i$ is

$$\frac{\mathrm{d}\mathbf{r}_i}{\mathrm{d}t} = \mu\mathbf{E}(r_i) + \sum_{j=1}^{N}\frac{\partial \mathbf{D}_{ij}}{\partial \mathbf{r}_j} + \sum_{j=1}^{N}\frac{\mathbf{D}_{ij}\cdot(\mathbf{F}_j^{\mathrm{es}} + \mathbf{F}_j^{\mathrm{ev}} + \mathbf{F}_j^{\mathrm{wall}})}{k_{\mathrm{B}}T} + \left(\frac{6}{\Delta t}\right)^{1/2}\sum_{j=1}^{i}\mathbf{B}_{ij}\cdot\mathbf{n}_j \quad (1)$$

where $\mu$ is the mobility of DNA, $\mathbf{r}_i$ the coordinate vector of bead $i$, $\mathbf{E}$ the electric field, $\mathbf{D}_{ij}$ the mobility tensor, $\mathbf{F}_j^{\mathrm{es}}$ the

effective spring force, $\mathbf{F}_j^{\mathrm{ev}}$ the excluded volume force to prevent unrealistic crossings and collisions between beads, $\mathbf{F}_j^{\mathrm{wall}}$ the repulsion force caused by the hyperbolic contraction walls, $k_{\mathrm{B}}$ the Boltzmann constant, $T$ the absolute temperature, $\Delta t$ the time step, $\mathbf{B}_{ij}$ the coefficient tensor, and $\mathbf{n}_j$ is a random vector uniformly distributed in each of the three directions over the interval $[-1,1]$.

Hydrodynamic interaction is introduced into the stochastic differential equations through the mobility tensor $\mathbf{D}_{ij}$. In our model, the Rotne–Prager tensor is used [48].

$$\mathbf{D}_{ij} = \frac{k_{\mathrm{B}}T}{6\pi\eta a}\mathbf{I}_{3\times 3} \quad \text{if} \quad i = j \tag{2}$$

$$\mathbf{D}_{ij} = \frac{k_{\mathrm{B}}T}{8\pi\eta r_{ij}}\left[\left(\mathbf{I}_{3\times 3} + \frac{\mathbf{r}_{ij}\mathbf{r}_{ij}}{r_{ij}^2}\right) + \frac{2a^2}{r_{ij}^2}\left(\frac{1}{3}\mathbf{I}_{3\times 3} - \frac{\mathbf{r}_{ij}\mathbf{r}_{ij}}{r_{ij}^2}\right)\right] \quad \text{if} \quad i \neq j \quad \text{and} \quad r_{ij} > 2a \tag{3}$$

$$\mathbf{D}_{ij} = \frac{k_{\mathrm{B}}T}{6\pi\eta a}\left[\left(1 - \frac{9}{32}\frac{r_{ij}}{a}\right)\mathbf{I}_{3\times 3} + \frac{3}{32}\frac{\mathbf{r}_{ij}\mathbf{r}_{ij}}{a r_{ij}}\right] \quad \text{if} \quad i \neq j \quad \text{and} \quad r_{ij} \leq 2a \tag{4}$$

where $\eta$ is the solvent viscosity, $a$ the radius of the beads, $\mathbf{r}_{ij} = \mathbf{r}_i - \mathbf{r}_j$, $r_{ij} = \|\mathbf{r}_{ij}\|$, and $\mathbf{I}_{3\times 3}$ is the identity tensor.

In addition, the coefficient tensor $\mathbf{B}_{ij}$ is related to the mobility tensor $\mathbf{D}_{ij}$ by:

$$\mathbf{D}_{ij} = \sum_{l=1}^{N} \mathbf{B}_{il}\cdot\mathbf{B}_{jl} \tag{5}$$

The mobility tensor is supposed to be symmetric and positive-definite, a Cholesky decomposition can be made between $\mathbf{D}_{ij}$ and $\mathbf{B}_{ij}$ as follows:

$$B_{ij} = \begin{cases} \left(D_{ij} - \sum_{k=1}^{j-1} B_{ik}B_{jk}\right)\Big/ B_{jj} & \text{if} \quad i > j \\ \left(D_{ii} - \sum_{k=1}^{i-1} B_{ik}^2\right)^{1/2} & \text{if} \quad i = j \\ 0 \quad \text{if} \quad i < j \end{cases} \tag{6}$$

The effective spring force, $\mathbf{F}_j^{\mathrm{es}}$, is given by

$$\mathbf{F}_j^{\mathrm{es}} = \begin{cases} \mathbf{F}_1^{\mathrm{s}} & \text{if} \quad j = 1 \\ \mathbf{F}_j^{\mathrm{s}} - \mathbf{F}_{j-1}^{\mathrm{s}} & \text{if} \quad 1 < j < N \\ \mathbf{F}_{N-1}^{\mathrm{s}} & \text{if} \quad j = N \end{cases} \tag{7}$$

where $\mathbf{F}_j^{\mathrm{s}}$ is the spring force associated with spring $j$. In our model, the Pade approximation is used to model the inverse Langevin force law [49]:

$$\mathbf{F}_j^{s} = \frac{k_B T}{b_{\mathrm{K}}}\frac{\mathbf{Q}_j}{Q_0}\left[\frac{3 - (Q/Q_0)^2}{1 - (Q/Q_0)^2}\right] \tag{8}$$

where $\mathbf{Q}_j = \mathbf{r}_{j+1} - \mathbf{r}_j$ is the spring connector vector for spring $j$, $Q$ the magnitude of $\mathbf{Q}_j$, $Q_0$ the maximum extensibility of each spring, and $b_{\mathrm{K}}$ is the Kuhn length which is twice the persistence length $l^{\mathrm{p}}$, i.e. $b_{\mathrm{K}} = 2l^{\mathrm{p}}$.

Excluded volume interactions are incorporated into our model to capture good solvents of DNA in aqueous solution. In the form of Gaussian coils, the excluded volume potential between two beads of the chain can be expressed as [39,40,50]:

$$U_{ij}^{\mathrm{ev}} = \frac{1}{2}\nu k_{\mathrm{B}}T N_{\mathrm{k,s}}^2\left(\frac{3}{4\pi S_{\mathrm{s}}^2}\right)^{3/2}\exp\left[\frac{-3r_{ij}^2}{4S_{\mathrm{s}}^2}\right] \tag{9}$$

where $\nu$ is the excluded volume parameter, $N_{\mathrm{k,s}}$ the number of Kuhn segments per spring, and $S_{\mathrm{s}} = \sqrt{(N_{\mathrm{k,s}}b_{\mathrm{K}}^2)/6}$ is the radius of gyration of each submolecule.

To realize the physical confinement of hyperbolic contraction walls, a bead-wall repulsive potential is introduced [38]:

$$U_j^{\mathrm{wall}} = \begin{cases} \frac{A_{\mathrm{wall}}}{3b_{\mathrm{K}}\delta_{\mathrm{wall}}^2}(h - \delta_{\mathrm{wall}})^3 & \text{if} \quad h < \delta_{\mathrm{wall}} \\ 0 \quad \text{if} \quad h > \delta_{\mathrm{wall}} \end{cases} \tag{10}$$

where $h$ is the distance of bead $j$ from the wall in the wall-normal direction, $\delta_{\mathrm{wall}}$ the cut-off distance, and $A_{\mathrm{wall}}$ is the repulsive energy constant. In our model, we use $A_{\mathrm{wall}} = 25k_{\mathrm{B}}T$ and $\delta_{\mathrm{wall}} = b_{\mathrm{K}}N_{\mathrm{k,s}}^{1/2}/2$.

Forces on bead $j$ due to excluded volume effect and molecule-wall repulsion can be obtained from the usual relation, $\mathbf{F}_j = -\nabla_j\mathbf{U}$.

### 3.2. Numerical scheme and parameters

The available simple techniques for integrating Eq. (1) are explicit forward Euler integration scheme and semi-implicit Newton's scheme [51]. Small time-step is required for the Euler integration scheme in order to reproduce the accurate results, which results in a very long simulation run time. A semi-implicit Newton's scheme is also becomes time consuming as the chain size becomes large, due to heavy computational load in iteration at every time-step. The more CPU efficient "predictor–corrector" method is used in this paper. "Predictor–corrector" method is first introduced by Öttinger to promise higher accuracy and less simulation run time [52,53]. Somasi et al. modified this method into three-step "predictor–corrector" method [54] and Heieh et al. took the hydrodynamic interaction into account for calculations [55]. Rewriting the Eq. (1) in terms of the spring vectors $\mathbf{Q}$ rather than the bead position $\mathbf{r}$ is as following:

$$\mathbf{Q}_i^{t+\Delta t} = \mathbf{Q}_i^t + \left\{\mu\left[\mathbf{E}\left(r_{i+1}^t\right) - \mathbf{E}\left(r_i^t\right)\right] + \sum_{j=1}^{N}\frac{(\mathbf{D}_{i+1,j}^t - \mathbf{D}_{i,j}^t)\cdot(\mathbf{F}_j^{\mathrm{s},t} - \mathbf{F}_{j-1}^{\mathrm{s},t} + \mathbf{F}_j^{\mathrm{ev}} + \mathbf{F}_j^{\mathrm{wall}})}{k_{\mathrm{B}}T} + \left(\frac{6}{\Delta t}\right)^{1/2}\sum_{j=1}^{i}(\mathbf{B}_{i+1,j}^t - \mathbf{B}_{i,j}^t)\cdot\mathbf{n}_j\right\}\cdot\Delta t \tag{11}$$

where $\mathbf{Q}_i$ is $i$th spring vector, and $\Delta t$ is the time step.

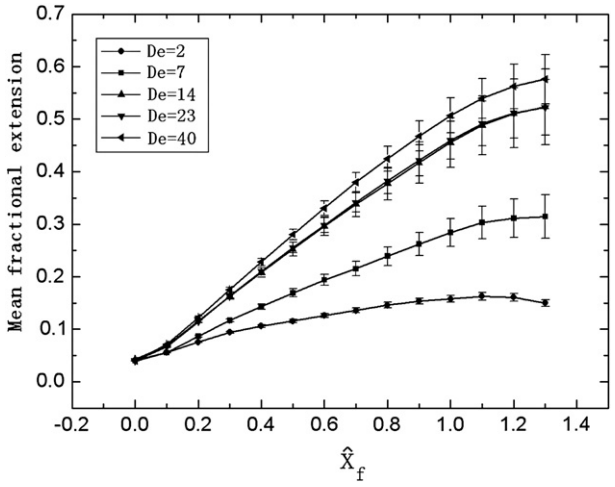


Fig. 2. Plots of mean fractional extension against the $x$-coordinate of the front of the DNA $\hat{x}_f = x_f/l_c$ in a hyperbolic contraction microchannel for various De.

The three-step ''predictor–corrector'' method consists of one predictor and two corrector steps. Details of the algorithm can be found in the Refs. [54,55].

Polymers were driven by electric field through the microchannel with detailed parameters: $l_1 = 1.5$ mm, $l_2 = 1.52$ mm, $l_3 = 1.5$ mm, $l_c = 80$ μm, $h_1 = 200$ μm, $h_2 = 3.8$ μm, $h_3 = 200$ μm, $c = 155$ μm$^2$. Due to the sharper gradient of electric potential, the maximum element size on the hyperbolic contraction walls is $1 \times 10^{-6}$, while $2 \times 10^{-5}$ in other regions.

Thirty initial conformations were recorded under no-flow conditions. The 169 kbp of T4 DNA is modeled as 35 beads with the radius of each beads 77 nm connected by 34 springs, where the length of each spring corresponds to the product of the Kuhn length, 106 nm, and the number of Kuhn segments per spring, 19.8. In the Brownian dynamics simulations, we set the excluded volume parameter, $\nu = 0.0012$ μm$^3$.

Two natural time scales, where one is the longest relaxation time of polymer $\tau$, the other is the inverse of strain rate $1/\dot{\varepsilon}$, are related through the Deborah number: $\mathrm{De} = \dot{\varepsilon}\tau = \mu E_2 \tau / l_c$, where $\mu$ is the measured electrophoretic mobility of the T4 DNA, and $E_2$ is the maximum electric field strength at the contraction exit. By fitting the relaxation data to an exponential decay [36]:

$$\left\langle x_{(t)}^2 \right\rangle = A \exp(-t/\tau) + B \tag{12}$$

where $\langle x_{(t)} \rangle$ is defined as the distance between the downstream-most part of the molecule and the upstream-most part, $A$ the fitting parameter, and $B$ corresponds to the mean square coil size at equilibrium. We obtain the relaxation time, $\tau = 0.8$ s, in an unrestricted state. The higher value 1.7 s is used in the actual simulations due to the restriction of microchannel [21].

## 4. Results and discussions

### 4.1. Effect of Deborah number

In this paper, the electric potential is applied on the both ends of a microchannel. T4 DNA moves to the hyperbolic contraction from the right inlet. The mean fractional extensions of T4 DNA against the $x$-coordinate of the front of the DNA $\hat{x}_f = x_f/l_c$ at De = 2, 7, 14, 23, and 40 are shown in Fig. 2. It can be found, from Fig. 2, that the increase in De leads to higher extensions of T4 DNA in a hyperbolic contraction microchannel.

Fig. 3 shows 30 individual fractional extensions $\hat{x}_{ex} = x_{ex}/L$ as a function of $\hat{x}_f$ at De = 2 and De = 23. We can find from Fig. 3(a) that the individual fractional extensions are very small and the curves appear to oscillate in degree of stretch. In this microchannel, the strain rate is inhomogeneous. While at De = 2, the strain rate is just above the stretching critical value only in the small region of hyperbolic contraction. As a result, the random Brownian fluctuation plays an important role in the stretching dynamics, when the Deborah numbers are low.

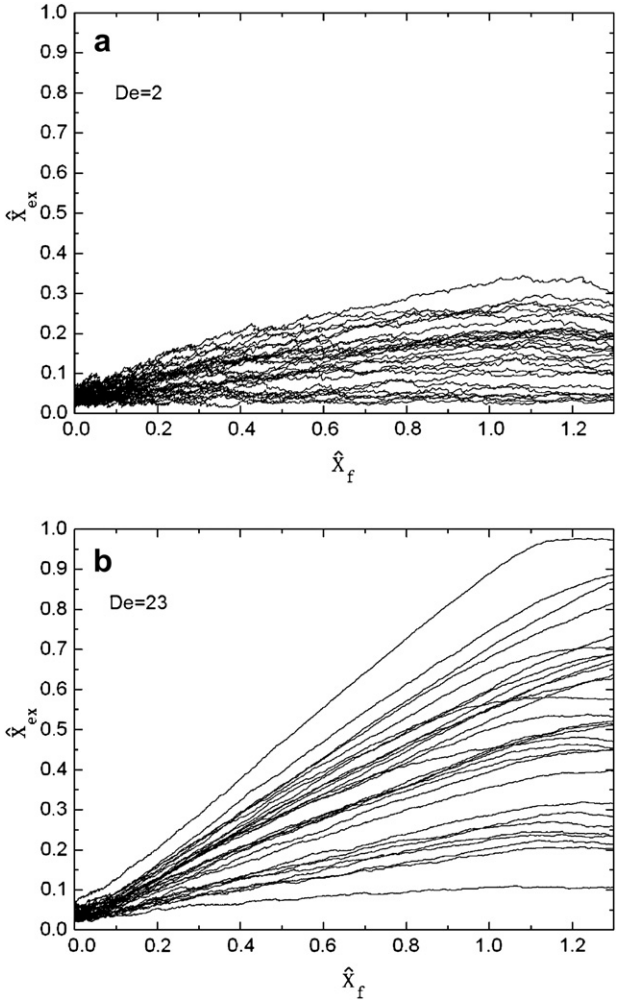


Fig. 3. Plots of 30 individual fractional extensions $\hat{x}_{ex} = x_{ex}/L$ as a function of $\hat{x}_f = x_f/l_c$ in a hyperbolic contraction microchannel for (a) De = 2 and (b) De = 23.

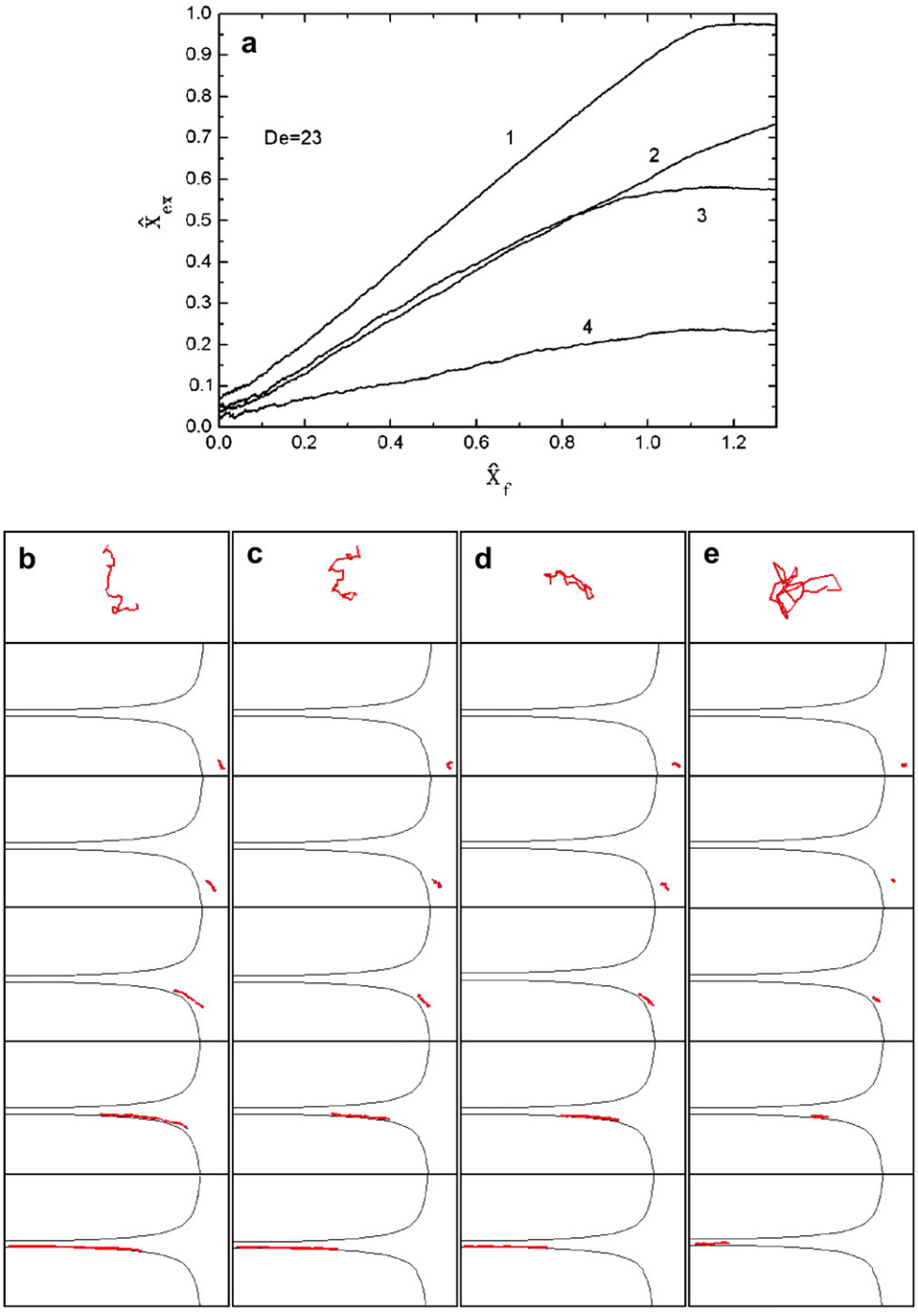


Fig. 4. Comparison of stretching dynamics for four initial conformations: (a) individual fractional extension $\widehat{x}_{ex}$ versus $\widehat{x}_f$; (b) single-dumbbell initial conformation; (c) kinked initial conformation; (d) folded initial conformation and (e) coiled initial conformation.

In the case of high De (De = 23), the stretching behavior shown in Fig. 3(b) is stronger than that at lower De values, but the oscillations in these curves still can be found. Some curves show rapid extensions and other curves show slow extensions, which indicate that different initial conformation of T4 DNA may develop different stretching process. There is an obvious low stretching curve in which the molecule does not stretch at all. Scrutinizing this molecule shows us that the initial conformation appears to be in a coiled state. In addition, there are a few curves with an approximate plateau extension, where they show strong stretch early on, but don't extend any more at a later time. The competitive effects of the strain rate, the initial conformation and the Brownian fluctuations decide the degree of stretching of molecules.

The stretching behaviors in Figs. 2 and 3 indicate good qualitative agreement between our numerical predictions and experimental results. Quantitative comparisons show us that our mean fractional extension seems to be lower than experimental average stretch [21]. We attribute this difference primarily to the variation in initial chosen conformations.

### 4.2. Effect of initial conformation

We find that the stretching dynamics is sensitive to the starting conformation of the molecule. In order to illustrate this individualistic stretching, we consider the four typical initial configurations as shown in Fig. 4. The higher De is a better choice, where the influence of the starting conformation becomes more important and the effect of the Brownian fluctuation gets more trivial.

The polymer stretching dynamics in Fig. 4(b) corresponds to the Curve 1 in Fig. 4(a). This initial conformation can be considered as single-dumbbell where one of the ends of the molecule appears to be more coiled than in the other region. It is clear that this molecule is rapidly stretched to its steady-state extension.

The Curve 2 in Fig. 4(a) is representative of the stretching process in Fig. 4(c). On the whole, the starting conformation in Fig. 4(c) is more kinked than the single-dumbbell conformation in Fig. 4(b). In this hyperbolic microchannel, the stretching of this kinked molecule is also rapid but seems to be less extended than that of dumbbell state.

The Curve 3 in Fig. 4(a) represents the individual fractional extension of a folded molecule as shown in Fig. 4(d). This folded molecule can unravel rapidly until it reaches the metastable state where the force on one end counteracts that on the other end.

The stretching of coiled molecule in Fig. 4(e) corresponds to the Curve 4 in Fig. 4(a). It can be seen from Fig. 4(e) that the coiled molecule cannot unravel completely in the limit of finite De.

### 4.3. Effect of hydrodynamic interaction

To assess the effect of hydrodynamic interactions on the stretching dynamics, the cases with and without hydrodynamic interactions can be straightforwardly compared. The computational results of mean fractional extension at $\widehat{x}_f = 1$ for various Deborah numbers are presented in Fig. 5. It can be seen, from Fig. 5, that the full non-draining model and freely-draining model predict similar mean fractional extension.

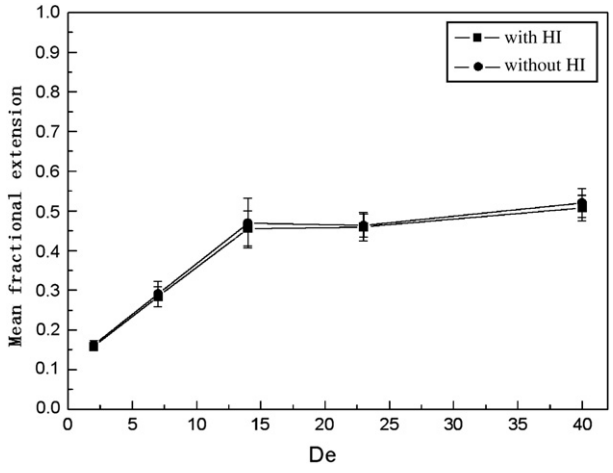


Fig. 5. Comparison of mean fractional extension at $\widehat{x}_f = 1$ as a function of De for the full non-draining model (with HI) and freely-draining model (without HI).

Hydrodynamic interactions have weak effect on the polymer stretching dynamics. This may be attributed to the screening effect in the confined geometry, which has been noted in the literatures [56,57]. The other important reason may be that the effect of hydrodynamic interactions on the stretching behaviors of molecules has been absorbed into the Deborah number. The latter explanation is similar to the conclusion of Winkler [28], where the Weissenberg number has involved the influence of the hydrodynamic interactions on the structural and dynamical properties of semiflexible polymers in shear flow.

## 5. Conclusion

The bead-spring Brownian dynamics is used to simulate the stretching dynamics of T4 DNA in hyperbolic contraction microchannels.

The simulations show that the stretching dynamics depend on the competitive effect of the strain rate, the Brownian fluctuation and the initial conformation. A higher De value can lead to more rapid and increasing extension. In the case of low De, the influence of Brownian fluctuations is more prominent. In the case of high De, the initial conformation of a molecule have strong effect on the stretching process, where the dumbbell-shaped molecule can stretch most rapidly and the coiled molecule can extend most slowly, the folded molecule may unravel until it reaches the metastable state.

Much attention has been paid in this paper to the hydrodynamic interactions. The involvement of Deborah number and the screening effect caused by the confinement of microchannels lead to the weak dependence of mean fractional extension on the hydrodynamic interactions.

The present study shows the strong ability to predict the microscopic dynamics of polymers and can be extended to other fields of microchannels.

## Acknowledgements

This work is supported by the Chinese National Natural Science Foundation Grant No. 10572053, the Doctor Foundation Grant No. 20040183057, and the Chinese National Programs for High Technology Research and Development Grant No. 2006AA04Z305.

## References

[1] Smith SB, Cui Y, Bustamante C. Overstretching B-DNA: the elastic response of individual double-stranded and single-stranded DNA molecules. Science 1996;271:795–9.
[2] Simmons RM, Finer JT, Chu S, Spudich JA. Quantitative measurements of force and displacement using an optical trap. Biophys J 1996;70:1813–22.
[3] Amblard F, Yurke B, Pargellis A, Leibler S. A magnetic manipulator for studying local rheology and micromechanical properties of biological systems. Rev Sci Instrum 1996;67(3):818–27.
[4] Cluzel P, Lebrun A, Heller C, Lavery R, Viovy JL, Chatenay D, et al. DNA: an extensible molecule. Science 1996;271:792–4.

[5] Schwartz DC, Li X, Hernandez LI, Ramnarain SP, Huff EJ, Wang YK. Ordered restriction maps of Saccharomyces cerevisiae chromosomes constructed by optical mapping. Science 1993;62:110–4.
[6] Petit CAP, Carbeck JD. Combing of molecules in microchannels (COMMIC): a method for micropatterning and orienting stretched molecules of DNA on a surface. Nano Lett 2003;3:1141–6.
[7] Michalet X, Ekong R, Fougerousse F, Rousseaux S, Schurra C, Hornigold N, et al. Dynamic molecular combing: stretching the whole human genome for high-resolution studies. Science 1997;277:1518–23.
[8] Dimalanta ET, Lim A, Runnheim R, Lamers C, Churas C, Forrest DK, et al. A microfluidic system for large DNA molecule arrays. Anal Chem 2004;76:5293–301.
[9] Aston C, Hiort C, Schwartz DC. Optical mapping: an approach for fine mapping. Methods Enzymol 1999;303:55–73.
[10] Tegenfeldt JO, Prinz C, Cao H, Chou S, Reisner WW, Riehn R, et al. From the cover: the dynamics of genomic-length DN molecules in 100-nm channels. Proc Natl Acad Sci USA 2004;101:10979–83.
[11] Li W, Tegenfeldt JO, Chen L, Austin RH, Chou SY, Kohl P, et al. Sacrificial polymers for nanofluidic channels in biological applications. Nanotechnology 2003;14:578–83.
[12] Riehn R, Lu M, Wang YM, Lim SF, Cox EC, Austin RH. Restriction mapping in nanofluidic devices. Proc Natl Acad Sci USA 2005;102: 10012–6.
[13] Perkins TT, Smith DE, Larson RG, Chu S. Stretching of a single tethered polymer in a uniform flow. Science 1995;268:83–7.
[14] Tegenfeldt JO, Bakajin O, Chou CF, Chan SS, Austin R, Fann W, et al. Near-field scanner for moving molecules. Phys Rev Lett 2001;86(7): 1378–81.
[15] Larson JW, Yantz GR, Zhong Q, Charnas R, D'Antoni CM, Gallo MV, et al. Single DNA molecule stretching in sudden mixed shear and elongational microflows. Lab Chip 2006;6:1187–99.
[16] Chan EY, Goncalves NM, Haeusler RA, Hatch AJ, Larson JW, Maletta AM, et al. DNA mapping using microfluidic stretching and single-molecule detection of fluorescent site-specific tags. Genome Res 2004;14(6):1137–46.
[17] Wong PK, Lee Y-K, Ho C-M. Deformation of NA molecules by hydrodynamic focusing. J Fluid Mech 2003;497:55–65.
[18] Ferree S, Blanch HW. Electrokinetic stretching of tethered DNA. Biophys J 2003;85:2539–46.
[19] Randall GC, Doyle PS. Electrophoretic collision of a DNA molecule with an insulating post. Phys Rev Lett 2004;93:058102.
[20] Randall GC, Doyle PS. DNA deformation in electric fields: DNA driven past a cylindrical obstruction. Macromolecules 2005;38:2410–8.
[21] Randall GC, Schultz KM, Doyle PS. Methods to electrophoretically stretch DNA: microcontractions, gels, and hybrid gel-microcontraction devices. Lab Chip 2006;6:516–25.
[22] Ueda M. Dynamics of long DNA confined by linear polymers. J Biochem Biophys Meth 1999;41(2–3):153–65.
[23] Kaji N, Ueda M, Baba Y. Molecular stretching of long DNA in agarose gel using alternating current electric fields. Biophys J 2002;82:335–44.
[24] Kaji N, Ueda M, Baba Y. Stretching of megabase-sized deoxyribonucleic acid molecules by tuning electric-field frequency. Appl Phys Lett 2003;83(16):3413–5.
[25] Namasivayam V, Larson RG, Burke DT, Burns MA. Electrostretching DNA molecules using polymer-enhanced media within microfabricated devices. Anal Chem 2002;74:3378–85.
[26] Hofmann T, Winkler RG, Reineker P. Dynamics of a polymer chain in an elongational flow. Phys Rev E 2000;61:2840–7.
[27] Ripoll M, Winkler RG, Gompper G. Star polymers in shear flow. Phys Rev Lett 2006;96:188302.
[28] Winkler RG. Semiflexible polymers in shear flow. Phys Rev Lett 2006; 97:128301.
[29] Petera D, Muthukumar M. Brownian dynamics simulation of bead–rod chains under shear with hydrodynamic interaction. J Chem Phys 1999;111(16):7614–23.
[30] Liu S, Ashok B, Muthukumar M. Brownian dynamics simulations of bead-rod-chain in simple shear flow and elongational flow. Polymer 2004;45(4):1383–9.
[31] Kim JM, Doyle PS. A Brownian dynamics-finite element method for simulating DNA electrophoresis in nonhomogeneous electric fields. J Chem Phys 2006;125:074906.
[32] Streek M, Schmid F, Duong TT, Anselmetti D, Ros A. Two-state migration of DNA in a structured microchannel. Phys Rev E 2005;71:011905.
[33] Panwar AS, Kumar S. Time scales in polymer electrophoresis through narrow constrictions: a brownian dynamics study. Macromolecules 2006;39(3):1279–89.
[34] Kim JM, Doyle PS. Design and numerical simulation of a DNA electrophoretic stretching device. Lab Chip 2007;7:213–25.
[35] Panwar AS, Kumar S. Brownian dynamics simulations of polymer stretching and transport in a complex electroosmotic flow. J Chem Phys 2003;118(2):925–36.
[36] Larson RG, Hu H, Smith DE, Chu S. Brownian dynamics simulations of a DNA molecule in an extensional flow field. J Rheol 1999;43(2):267–304.
[37] Hur JS, Shaqfeh ESG, Babcock HP, Chu S. Dynamics and configurational fluctuations of single DNA molecules in linear mixed flows. Phys Rev E 2002;66(1):011915.
[38] Jendrejack RM, Schwartz DC, de Pablo JJ, Graham MD. Shear-induced migration in flowing polymer solutions: simulation of long-chain DNA in microchannels. J Chem Phys 2004;120(5):2513–29.
[39] Jendrejack RM, Pablo JJd, Graham MD. Stochastic simulations of DNA in flow: dynamics and the effects of hydrodynamic interactions. J Chem Phys 2002;116(17):7752–9.
[40] Jendrejack RM, Schwartz DC, Graham MD, de Pablo JJ. Effect of confinement on DNA dynamics in microfluidic devices. J Chem Phys 2003;119(2):1165–73.
[41] Tessier F, Labrie J, Slater GW. Electrophoretic separation of long polyelectrolytes in submolecular-size constrictions: a Monte Carlo study. Macromolecules 2002;35(12):4791–800.
[42] Perkins TT, Smith DE. Single polymer dynamics in an elongational flow. Science 1997;276(5321):2016–21.
[43] Smith DE, Chu S. Response of flexible polymers to a sudden elongational flow. Science 1998;281:1335–40.
[44] Larson RG, Magda JJ. Coil-stretch transitions in mixed shear and extensional flows of dilute polymer solutions. Macromolecules 1989;22(7):3004–10.
[45] Long D, Viovy J-L, Ajdari A. Simultaneous action of electric fields and nonelectric forces on a polyelectrolyte: motion and deformation. Phys Rev Lett 1996;76(20):3858–61.
[46] Long D, Viovy J-L, Ajdari A. Stretching DNA with electric fields revisited. Biopolymers 1996;39:755–9.
[47] Ermak DL, McCammon JA. Brownian dynamics with hydrodynamic interactions. J Chem Phys 1978;69(4):1352–60.
[48] Rotne J, Prager S. Variational treatment of hydrodynamic interaction in polymers. J Chem Phys 1969;50(11):4831–7.
[49] Cohen A. A Padé approximant to the inverse Langevin function. Rheol Acta 1991;30(3):270–3.
[50] Schroeder CM, Shaqgeh ESG, Chu S. Effect of hydrodynamic interactions on DNA dynamics in extensional flow: simulation and single molecule experiment. Macromolecules 2004;37:9242–56.
[51] Jendrejack RM, Graham MD, de Pablo JJ. Hydrodynamic interactions in long chain polymers: application of the Chebyshev polynomial approximation in stochastic simulations. J Chem Phys 2000;113(7):2894–900.
[52] Öttinger HC. Stochastic processes in polymeric fluids. Berlin: Springer; 1996.
[53] Herrchen M, Öttinger HC. A detail comparison of various FENE dumbbell models. J Non-Newtonian Fluid Mech 1997;68:17–42.
[54] Somasi M, Khomami B, Woo NJ, Hur JS, Shaqfeh ESG. Brownian dynamics simulations of bead-rod and bead-spring chains: numerical algorithms and coarse-graining issues. J Non-Newtonian Fluid Mech 2002;108(1–3):227–55.
[55] Hsieh CC, Li L, Larson RG. Modeling hydrodynamic interaction in Brownian dynamics: simulations of extensional flows of dilute solutions of DNA and polystyrene. J Non-Newton Fluid 2003;113(2–3):147–91.
[56] Bakajin OB, Duke TAJ, Chou CF, Chan SS, Austin RH, Cox EC. Electrohydrodynamic stretching of DNA in confined environments. Phys Rev Lett 1998;80:2737–40.
[57] Balducci A, Mao P, Han J, Doyle PS. Double-stranded DNA diffusion in slit-like nanochannels. Macromolecules 2006;39:6273–81.